CHIN. PHYS. LETT. Vol. 36, No. 11 (2019) 117801

Transient Photoconductivity in $LaRhO_3$ Thin Film *

Zhi Meng(孟智)[1,2], Lei Shen(沈磊)[1,2], Zongwei Ma(马宗伟)[1], Muhammad Adnan Aslam[1,2], Liqiang Xu(徐立强)[2], Xueli Xu(许学莉)[1,2], Wang Zhu(朱旺)[1], Long Cheng(成龙)[1,2], Yuecheng Bian(卞跃成)[1,2], Li Pi(皮雳)[1], Chun Zhou(周春)[1**], Zhigao Sheng(盛志高)[1**]

[1] *Anhui Province Key Laboratory of Condensed Matter Physics at Extreme Conditions, High Magnetic Field Laboratory, Chinese Academy of Sciences, Hefei 230031*

[2] *University of Science and Technology of China, Hefei 230026*

(Received 23 July 2019)

High-quality epitaxial $LaRhO_3$ (LRO) thin films on $SrTiO_3$ (110) single-crystalline substrates are fabricated by pulsed laser deposition and their photoconductivity properties are studied. The transient photoconductivity (TPC) effect is found in this semiconductor LRO film at room temperature. The magnitude of TPC increases almost linearly with the laser power intensities and the photon energies in visible light range. Moreover, the difference in the TPC results under two airflow conditions confirms that both intrinsic photoinduced carrier accumulation and extrinsic photoinduced heating effects contribute to the magnitude of TPC effect.

PACS: 78.20.−e, 81.15.Fg, 07.07.Df DOI: 10.1088/0256-307X/36/11/117801

Due to the complex coupling between spin, charge, lattice and orbital, transition metal oxides (TMOs) are generally sensitive to the external stimulation such as magnetic field, light and electric field.[1−4] Among them, photoinduced effect, such as photoconductivity, is especially interesting from the viewpoint of applications. Similar to the other property investigation, the photoconductivity effect was studied mostly in 3*d* transition metal oxides (3*d* TMOs), in which the outermost electron of transition metal element belongs to 3*d* orbital.[5−8]

In addition to 3*d* TMOs, $LaRhO_3$ (LRO) is an important prototype component in the catalog of 4*d* transition metal oxides (4*d* TMOs), in which the outermost electron of transition metal element belongs to 4*d* orbital, showing intriguing properties, such as paramagnetic insulator, thermopower and catalytic activity.[9−13] An LRO thin film as a p-type semiconductor active layer in an oxide photovoltaic device was also first reported in 2015.[14] However, very little information is available for the external stimulation induced physical properties of LRO so far. Hence, one may anticipate that there are some intriguing properties of the photoconductivity in LRO films.

In this work, high-quality LRO epitaxial thin films were grown and their photoconductivity effect was studied. Transient photoconductivity (TPC) was found in the LRO films at room temperature, and the laser power intensity and light wavelength dependences of TPC were also investigated. Moreover, the different results obtained under different airflow conditions indicate that both intrinsic photoinduced carrier accumulation and extrinsic photoinduced heating effects contribute to the magnitude of TPC.

The polycrystalline LRO target was prepared by solid-state reaction using La_2O_3 and Rh_2O_3 at 1200℃ in oxygen atmosphere. Since the Rh element is volatile, an excess of 5% Rh_2O_3 was added to the target. LRO thin films were grown by pulsed laser deposition (PLD) using a 248 nm KrF exciter laser and a pulse duration of 20 ns. The optimal growth parameters were growth temperature of 770℃, oxygen pressure of 5 Pa, and laser fluence of 1 J/cm^2. After deposition, the sample was cooled to room temperature under deposition pressure. Thereafter, *ex situ* annealing was performed at 650℃ for 3 h in an oxygen atmosphere of 1 atm to ensure complete and homogeneous oxygenation of the thin films. The structural characteristic was examined by a Panalytical X'pert high-resolution x-ray diffractometer. The electrical transport properties were measured using a manufactured multi-measurement system on a Janis 9 T magnet. The absorption spectra were measured using a UV-Vis-NIR spectrophotometer (Shimadzu UV3600-MPC3100). The photoconductive test system was established, in which the resistance was measured by a Keithley 2400 SourceMeter with constant current mode. The resistance is proportional to the voltage, thus the change in resistance is consistent with the change in voltage. Three laser wavelengths of 780, 532 and 473 nm were selected for illumination.

X-ray diffraction (XRD) measurement was performed to study the crystal quality of LRO thin film. Symmetric θ–2θ scan around the peak of the STO (110) substrate was exhibited to measure the out-of-plane lattice parameters of the thin film (Fig. 1(a)). The clear Kiessig fringes near the LRO Bragg reflection peak confirmed the high quality of the LRO thin film. The thickness of the LRO thin film is calculated to be about 35 nm.[15] According to the Bragg formula $2d\sin\theta = n\lambda$, the out-of-plane lattice constant of the thin film is 4.04 Å, which is larger than

*Supported by the National Key R&D Program of China under Grant Nos 2017YFA0303603 and 2016YFA0401803, the National Natural Science Foundation of China under Grant Nos 11574316, U1532155, 61805256 and U1832106, and the Key Research Program of Frontier Sciences of CAS under Grant No QYZDB-SSW-SLH011.

**Corresponding author. Email: zhigaosheng@hmfl.ac.cn; chun.zhou@hmfl.ac.cn

© 2019 Chinese Physical Society and IOP Publishing Ltd

the pseudocubic lattice constant of 3.96 Å, and the corresponding peak position is 31.9° (dashed line in Fig. 1(a)). As shown in Fig. 1(b), the temperature-dependent resistivity measurement result of the LRO thin film shows a semiconductor feature in the whole temperature range, just like its bulk counterpart.[16,17] In addition, the temperature (T) dependence of resistivity ρ can be fitted by a three-dimensional variable-range hopping (VRH) conduction mechanism,[18]

$$\rho = \rho_0 \exp(T/T_0)^{-1/4}, \tag{1}$$

where ρ_0 is the resistivity coefficient, and T_0 is the characterize temperature.[17] It is confirmed by the linear dependence of $\ln\rho$ on $T^{-1/4}$ (inset of Fig. 1(b)).

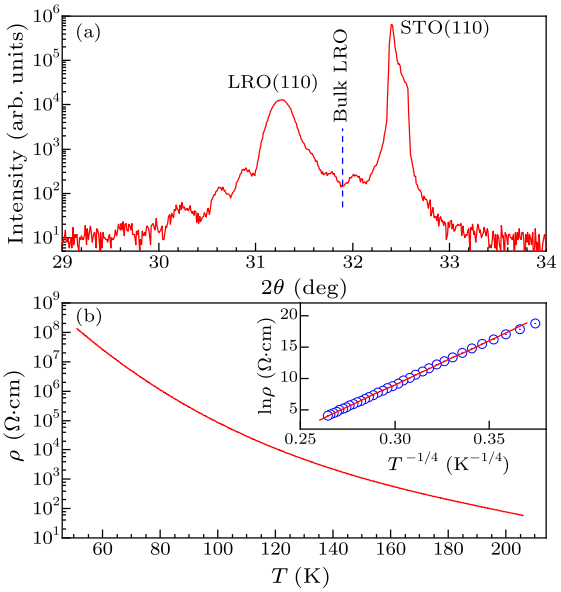

Fig. 1. Characterization of the LRO thin film. (a) XRD pattern of the LRO thin film, and (b) ρ–T curve of the LRO thin film. The fit of the resistivity data by the variable-range hopping model is shown in the inset.

The electrical transport property of the LRO thin film was not only measured in dark state (Fig. 1(b)) but also in light illumination state. The resistance and photoconductivity of the LRO thin film were measured, and the schematic of the experimental setup is shown in Fig. 2(a). The ohmic contacts were prepared by evaporating 50-nm-thick Au on the surface of the sample for electrodes with a designed pattern. The laser beam was focused on the middle of two electrodes to avoid illumination on the electrodes. Figure 2(b) shows that the resistance changes with time at a wavelength of 532 nm, laser power of 10 mW and 20 mW. The labels 'Laser on' and 'Laser off' indicate that the laser is turned on and off, respectively. In Fig. 2(b), when the thin film is exposed to illumination, the resistance drops instantaneously, and this initial drop gradually decreases over time during light exposure. After the laser is turned off, the resistance returns to the initial value, indicating the effect of transient photoconductivity (TPC). The TPC value can be calculated by

$$\mathrm{TPC} = [(R_\mathrm{d} - R_\mathrm{i}) * 100\%]/R_\mathrm{d}, \tag{2}$$

where R_d and R_i are the resistances of the LRO thin film in the dark and illumination state, respectively. The laser powers dependence of calculated TPC values are shown in Fig. 2(c). From the fitting result, the magnitude of TPC increases almost linearly with the laser power, which is similar to the previous reports.[19,20] In the experiment, we also changed the polarization of laser during the TPC measurement. The difference under s and p polarizations is small, and it is far less than the TPC of LRO thin film. Therefore, the effect of laser polarization on the TPC can be ignored.

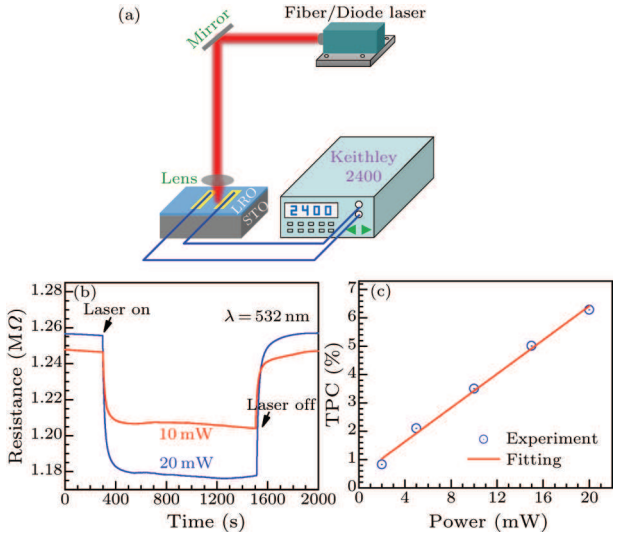

Fig. 2. Resistance of the LRO thin film changed with different laser powers at 532 nm. (a) Schematic of the TPC measurement system. Three laser sources were used in the experiment: a fiber laser with 780 nm and two diode lasers with 532 and 473 nm. (b) Time dependence of resistance with 10 mW and 20 mW. (c) TPC versus laser power.

In addition to the laser power dependence, the light wavelength effect on the TPC has also been studied at three different wavelengths of 780, 532 and 473 nm. The laser power was 20 mW since the TPC at 20 mW has an obvious response (see Fig. 2). In Fig. 3(a), the resistance decreases quickly after turning on the laser and achieves a constant value after a relaxation process. The relaxation times τ at the wavelengths of 780, 532 and 473 nm are 85, 93 and 99 s, respectively, where τ is defined as the time required for a 90% change in resistance after laser illumination.[21] It reflects the speed at which the equilibrium state is reached. The sample illuminated by the shorter wavelength has a smaller equilibrium resistance during the illumination. In particular, the wavelength of 473 nm corresponds to the highest TPC value of 6.6% (Fig. 3(b)). Furthermore, the tendency of TPC with wavelength is similar to the absorption spectrum of the LRO thin film. From the absorption spectrum, the linear extrapolation (dashed line) to the abscissa gets a band gap at 1.4 eV (886 nm). TPC values increase

almost linearly with the photon energies in the visible light range, as shown in Fig. 3(b). The TPC value changing with the wavelength (photon energy) can be also found in the previous reports.[5,22] For example, in the SnO_2 nanoribbon, illumination with 254 nm radiation results in a higher photoresponse than 365 nm radiation at both pure air and NO_2 atmosphere.[22]

The relationship between wavelength dependence of TPC and absorption spectrum is in good agreement. There are two possibilities for this phenomenon. First, short laser wavelengths have higher excitation efficiency for carriers, resulting in higher TPC. Second, the sample has a higher absorption coefficient in the short wavelength range,[14] and more laser energy will be converted into heat, resulting in a temperature increase. Since a higher temperature corresponds to smaller resistance, as shown in Fig. 1(b), the sample illuminated by a shorter wavelength will have a higher TPC. It is also noticed that the relaxation time of the sample is relatively long, nearly 100 s, which is longer than the relaxation time in the TPC studies of most TMOs.[3,23,24] These features indicate that there may exist photoinduced heating effect.

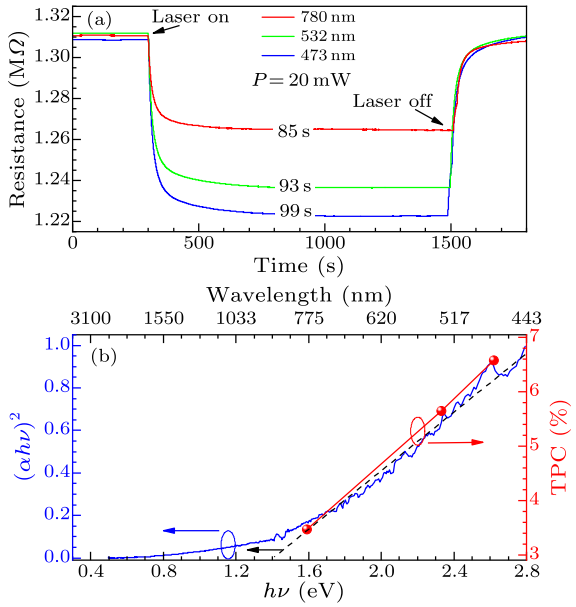

Fig. 3. (a) Resistance at three different wavelengths with the same laser power of 20 mW. The illumination time is 1200 s. Labels on the lines show the relaxation times. (b) TPC and $(\alpha h\nu)^2$ versus wavelength for the LRO thin films. The laser power is 20 mW. A linear extrapolation (dashed line) to the abscissa gives a band gap of 1.4 eV (886 nm).

The STO substrate has a band gap of 3.2 eV, which is higher than the photon energy we used, thus the sample substrate does not absorb photon energy. In addition, the band gap of the LRO thin film is 1.4 eV, which is smaller than the photon energy we used. If the photoinduced heating effect is active, then only the surface temperature of the sample will rise. To identify the existence of photoinduced heating effect, TPC effects were measured with surface cooling by blowing different airflows. The flowing gas would eliminate the thermal effect of the film and the absolute TPC value is expected to be reduced.

As shown in Fig. 4(a), we blow the sample surface at two airflow conditions: with compressed air (red line) and air (blue line), where the wavelength is 532 nm and the laser power is 20 mW. The initial resistance under compressed air is higher than that under normal air because blowing compressed air will take away heat from the sample surface compared to the sample in the natural air and raise its resistance. Figure 4(b) shows that the TPC effect at the flowing compressed air is reduced by 18%. As we all know, heat loss does not change the excited state and carrier concentration. Thus, the reduction of the TPC value in the LRO thin film comes from the thermal effect. Therefore, it can be deduced that in addition to the intrinsic photoinduced carrier accumulation effect, the photoinduced heating effect also plays an important role in the TPC of the LRO thin film.

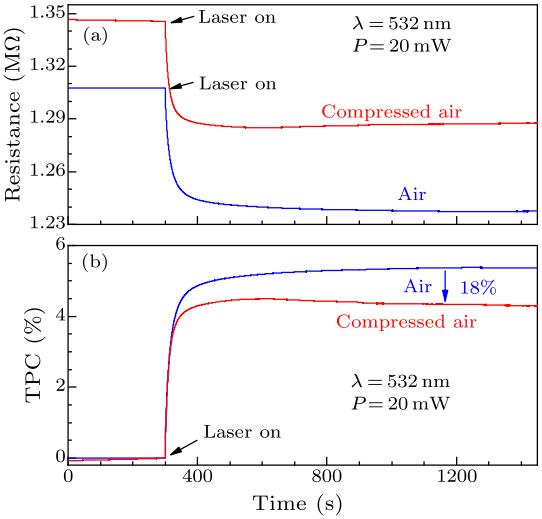

Fig. 4. There are two airflow conditions: compressed air and normal air. (a) Time dependence of resistance. (b) Time dependence of TPC under the two conditions.

In conclusion, we have grown high-quality LRO thin films on STO (110) substrates and the TPC effect is studied. The laser power and photo energy dependence of TPC are characterized, and they both show a linear relationship. Under different airflow conditions, the TPC shows different behaviors, which indicates that both intrinsic photoinduced carrier accumulation and extrinsic photoinduced heating effects contribute to the magnitude of TPC. The LRO thin films have many potential applications in creating optoelectronic devices, such as optical switchers and photodetectors.

References

[1] Vonhelmolt R, Wecker J, Holzapfel B, Schultz L and Samwer K 1993 *Phys. Rev. Lett.* **71** 2331
[2] Rastogi A, Kushwaha A K, Shiyani T, Gangawar A and Budhani R C 2010 *Adv. Mater.* **22** 4448
[3] Beyreuther E, Thiessen A, Grafström S, Eng L M, Dekker M C and Dörr K 2009 *Phys. Rev. B* **80** 075106

[4] Dao L Y, Zhang Z T, Xiao Y T, Zhang M H, Wang S, He J, Jia J S, Yu L J, Sun B and Xiong C M 2019 *Acta Phys. Sin.* **68** 067302 (in Chinese)
[5] Tsai S H, Basu S, Huang C Y, Hsu L C, Lin Y G and Horng R H 2018 *Sci. Rep.* **8** 14056
[6] Cauro R, Gilabert A, Contour J P, Lyonnet R, Medici M G, Grenet J C, Leighton C and Schuller I K 2001 *Phys. Rev. B* **63** 174423
[7] Kiryukhin V, Casa D, Hill J P, Keimer B, Vigliante A, Tomioka Y and Tokura Y 1997 *Nature* **386** 813
[8] Yan G Y, Zhang H L, Bai Z L, Wang S F, Wang J L, Yu W and Fu G S 2013 *Chin. Phys. Lett.* **30** 046801
[9] Taniguchi T, Iizuka W, Nagata Y, Uchida T and Samata H 2003 *J. Alloys Compd.* **350** 24
[10] Terasaki I, Shibasaki S, Yoshida S and Kobayashi W 2010 *Materials* **3** 786
[11] Shibasaki S, Takahashi Y and Terasaki I 2009 *J. Electron. Mater.* **38** 1013
[12] Gysling H J, Monnier J R and Apai G 1987 *J. Catal.* **103** 407
[13] Wold A, Post B and Banks E 1957 *J. Am. Chem. Soc.* **79** 6365
[14] Nakamura M, Krockenberger Y, Fujioka J, Kawasaki M and Tokura Y 2015 *Appl. Phys. Lett.* **106** 072103
[15] Pietsch U, Holy V and Baumbach T 2013 *High-Resolution X-ray Scattering: from Thin Films to Lateral Nanostructures* (Berlin: Springer)
[16] Mary T A and Varadaraju U V 1994 *J. Solid State Chem.* **110** 176
[17] Li Y J, Li S L, Gong P, Li Y L, Fang X Y, Jia Y H and Cao M S 2018 *Physica E* **104** 247
[18] Mott N F and Davis E A 1979 *Electronic Processes in Non-Crystalline Materials* 2nd edn (Oxford: Oxford University Press)
[19] Smolyaninova V N, Talanova E, Kennedy R, Kolagani R M, Overby M, Aldaco L, Yong G and Karki K 2007 *Phys. Rev. B* **76** 104423
[20] Li L, Auer E, Liao M, Fang X, Zhai T, Gautam U K, Lugstein A, Koide Y, Bando Y and Golberg D 2011 *Nanoscale* **3** 1120
[21] Deng Z, Meng G, Fang X, Dong W, Shao J, Wang S and Tong B 2019 *J. Alloys Compd.* **777** 52
[22] Law M, Kind H, Messer B, Kim F and Yang P 2002 *Angew. Chem. Int. Ed.* **41** 2405
[23] Chai X, Xing H and Jin K 2016 *Sci. Rep.* **6** 23280
[24] Takubo N, Ogimoto Y, Nakamura M, Tamaru H, Izumi M and Miyano K 2005 *Phys. Rev. Lett.* **95** 017404